HHS Public Access

Author manuscript

Angew Chem Int Ed Engl. Author manuscript; available in PMC 2018 June 01.

Published in final edited form as:

Angew Chem Int Ed Engl. 2017 June 01; 56(23): 6622–6626. doi:10.1002/anie.201701916.

Insights into how heme reduction potentials modulate enzymatic activities of a myoglobin-based functional oxidase

Dr. Ambika Bhagi-Damodaran[a], **Mr. Maximilian Kahle**[b], **Ms. Yelu Shi**[c], **Prof. Dr. Yong Zhang**[c], **Prof. Dr. Pia Ädelroth**[b], and **Prof. Dr. Yi Lu**[a]

[a]Department of Chemistry, University of Illinois at Urbana-Champaign, Urbana, IL. USA 61801

[b]Department of Biochemistry and Biophysics, Arrhenius Laboratories for Natural Sciences, Stockholm University, SE-10691 Stockholm, Sweden

[c]Department of Biomedical Engineering, Chemistry and Biological Sciences, Stevens Institute of Technology, Hoboken, New Jersey, NY. USA 07030

Abstract

Heme-copper oxidase (HCO) is a class of respiratory enzymes that use a heme-copper center to catalyze O_2 reduction to H_2O. While heme reduction potential ($E^{\circ\prime}$) of different HCO types has been found to vary >500 mV, its impact on HCO activity remains poorly understood. Here, we use a set of myoglobin-based functional HCO models to investigate the mechanism by which heme $E^{\circ\prime}$ modulates oxidase activity. Rapid stopped-flow kinetic measurements show that increasing heme $E^{\circ\prime}$ by ca. 210 mV results in increases in electron transfer (ET) rates by 30-fold, rate of O_2 binding by 12-fold, O_2 dissociation by 35-fold, while decreasing O_2 affinity by 3-fold. Theoretical calculations reveal that $E^{\circ\prime}$ modulation has significant implications on electronic charge of both heme iron and O_2, resulting in increased O_2 dissociation and reduced O_2 affinity at high $E^{\circ\prime}$ values. This work suggests fine-tuning $E^{\circ\prime}$ in HCOs and other heme enzymes can modulate their substrate affinity, ET rate and enzymatic activity.

TOC image

A four-electron reduction of O_2 to H_2O in heme-copper oxidase (HCO) requires an efficient control of electron transfer, O_2 binding/dissociation rates and O_2 affinity. By employing a functional model of HCO, we show that HCOs use their heme reduction potential to control these parameters, the electronics of bound O_2 and their overall enzymatic activity.

Correspondence to: Yong Zhang; Pia Ädelroth; Yi Lu.

A. B.-D. and M.K. contributed equally.

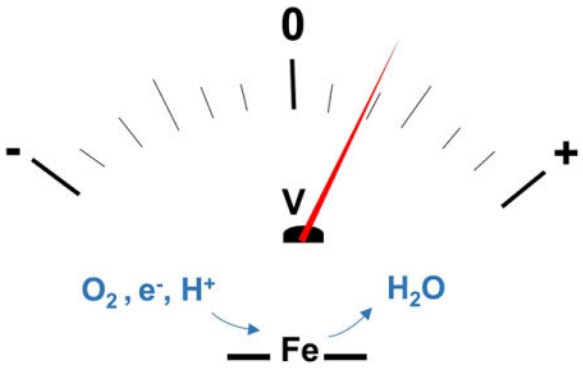

Keywords

Electron transfer; Heme proteins; Oxygen activation; Oxidoreductases; Redox chemistry

Heme proteins are a major class of metalloproteins that utilize the same cofactor, protoporphyrin IX, for a variety of functions including electron transfer (ET, as in cytochromes), storage and transfer of O_2 (as in myoglobin and hemoglobin), and O_2 activation (as in cytochrome P450).[1–3] A prime example of heme proteins is heme-copper oxidase (HCO) that catalyzes the kinetically challenging reduction of O_2 to H_2O and generates a trans-membrane proton gradient driving ATP synthesis.[4–7] The catalytic site of HCO, where O_2 reduction occurs, is a binuclear heme-copper center consisting of a high spin heme iron and a copper (Cu_B) coordinated to three histidines, one of which is cross-linked to a tyrosine residue. Despite this similarity, HCOs from different species use different heme types, such as heme *a*, *b*, and *o* at the catalytic heme center.[7] How different heme types impact biochemical properties HCOs is not understood. One such property is the reduction potential ($E^{\circ\prime}$) of the catalytic heme (Fe^{3+}/Fe^{2+}), which varies by ca. 500 mV in different HCO types (see Table S1 in SI).[8] Thus, question arises as to what is the origin for such variations of heme $E^{\circ\prime}$ and how does heme $E^{\circ\prime}$ impact HCO function. An efficient way to answer these questions is by systematically tuning heme $E^{\circ\prime}$ and probing resulting changes in functional activity. However, such manipulations are difficult in native HCOs due to their large size (~100–200 KDa), membranous nature and presence of multiple metal cofactors. To overcome these challenges, numerous small molecule models of HCOs have been designed,[9–10] but none to our knowledge have attempted to investigate the importance of heme $E^{\circ\prime}$ in regulating HCO function.

In an approach complementary to studying complex native enzymes and their small-molecule models, we use biosynthetic modelling, that utilizes smaller proteins/peptides as simpler synthetic models while retaining structural features of native enzymes.[11] We have designed biosynthetic structural and functional models of HCO in a smaller (17.4 KDa), easy-to-purify and soluble protein, myoglobin (Mb). To accomplish the goal, we first created a Cu_B-binding site in the distal pocket of Mb analogous to that in HCOs through L29H and F43H mutations to introduce two histidine ligands, that along with H64 complete the Cu_B coordination sphere.[12] We then introduced a tyrosine through F33Y mutation next to histidine ligands to model the conserved tyrosine in HCO.[13] The resultant mutant named

F33Y-Cu_BMb (Fig. 1A) mimicked HCOs functionally, as it could selectively reduce oxygen to water with hundreds of turnovers.[14] We further modulated heme $E^{\circ\prime}$ of F33Y-Cu_BMb by ~210 mV (Fig. 1B) *via* tuning of hydrogen bonding to heme iron (through S92A mutation) and using non-native heme cofactors with increased $E^{\circ\prime}$, such as monoformyl (MF-) and diformyl (DF-) hemes.[15] The F33Y-Cu_BMb variants, thus obtained namely, F33Y-Cu_BMb, S92A-F33Y-Cu_BMb, F33Y-Cu_BMb (MF-heme) and F33Y-Cu_BMb (DF-heme) exhibited systematic increase in $E^{\circ\prime}$ values of 95 ± 2 mV, 123 ± 3 mV, 210 ± 6 mV and 320 ± 10 mV respectively (all $E^{\circ\prime}$ reported in this work are vs. SHE). The increase in heme $E^{\circ\prime}$ for F33Y-Cu_BMb variants correlated with increases in their O_2 reduction activity (Fig. 2B). In particular, F33Y-Cu_BMb (DF-heme) with highest heme $E^{\circ\prime}$ displayed ca. 6-fold higher oxidase activity than parent F33Y-Cu_BMb.[15] In this work, we investigate the mechanism through which heme $E^{\circ\prime}$ impacts O_2 reduction activity of F33Y-Cu_BMb variants. Specifically, we focus on four key factors – ET rates, O_2 binding/dissociation rates and O_2 affinity – that can be modulated through tuning heme $E^{\circ\prime}$ and affect oxidase activity. Our results suggest that while the ET rates and O_2 binding/dissociation rates increase with increasing heme $E^{\circ\prime}$, the O_2 affinities decrease. Overall, the study shows that heme enzymes such as HCOs use heme $E^{\circ\prime}$ to control their substrate binding, electron transfer and enzymatic activities.

F33Y-Cu_BMb variants were expressed and purified without a copper at the Cu_B site. No copper was added in this work, as previous studies have shown that the presence of copper has little influence on the oxidase activity of F33Y-Cu_BMb.[14] To elucidate how $E^{\circ\prime}$ impacts enzymatic activity, we first probed variation in ET since tuning of $E^{\circ\prime}$ in metalloproteins is known to modulate their ET rates.[16–18] We reasoned that increasing $E^{\circ\prime}$ of heme such that it becomes higher than that of electron donor (N,N,N′,N′-tetramethyl-p-phenylenediamine, TMPD with $E^{\circ\prime}$ = 276 mV) may increase the driving force for ET. Increase in ET rates may then translate to higher O_2 reduction activity as previous reports on Mb-based HCO models revealed ET as the rate-limiting step in both enzymatic[19] and electrocatalytic[20] O_2 reduction reactions. To assess the role of ET, we measured the rate of reduction of Fe^{3+} to Fe^{2+} forms of F33Y-Cu_BMb variants using ascorbate ($E^{\circ\prime}$ = 90 mV) as a reductant and TMPD as a redox mediator. Owing to the strong and distinct spectroscopic signatures of heme iron in its Fe^{3+} and Fe^{2+} forms, we measured the rate of heme reduction by using stopped-flow absorption spectroscopy under strictly anaerobic conditions. Upon mixing 6 μM F33Y-Cu_BMb with 1500 eq. ascorbate and 150 eq. TMPD, we observed a rapid decrease in absorbance at 407 nm, 501 nm and 618 nm (corresponding to Fe^{3+} form) with a concomitant increase in absorbance at 434 nm and 556 nm (corresponding to Fe^{2+} form). The presence of isosbestic points in the spectra confirmed a clean transformation of Fe^{3+} to Fe^{2+} with no intermediate species (Fig. 2A). Fitting the absorbance change at 434 nm and 407 nm with time allowed us to determine the ET rate of F33Y-Cu_BMb as 0.10 ± 0.05/s. Similar experiments performed with other F33Y-Cu_BMb variants also displayed a clean transition from Fe^{3+} to Fe^{2+} form (Fig. S1). A plot of ET rates vs. heme $E^{\circ\prime}$, shown in Fig. 2B, indicates that as the heme $E^{\circ\prime}$ increases from 95 ± 2 mV to 123 ± 3 mV, 210 ± 6 mV and 320 ± 10 mV for F33Y-Cu_BMb, S92A-F33Y-Cu_BMb, F33Y-Cu_BMb (MF-heme) and F33Y-Cu_BMb (DF-heme) respectively, the ET rates increase correspondingly from 0.10 ± 0.005/s, to 0.19 ± 0.03/s, 0.76 ± 0.02/s, and 3.19 ± 0.07/s. This increase in ET is consistent

with the Marcus theory of electron transfer in a regime where $\Delta E°$ is lower than reorganization energy.[16] These results suggest that increasing heme $E°'$ in HCO mimics result in an increase in ET rates, which is potentially responsible for increase in O_2 reduction activity. However, the correlation between the two rates is not linear - While F33Y-Cu_BMb (MF-heme) and F33Y-Cu_BMb (DF-heme) exhibit 8-fold and 30-fold increase in ET rates as compared to F33Y-Cu_BMb, their oxidase activity increases only 4-fold and 5-fold respectively. Therefore, while fast ET is important to HCO activity, other factors such as O_2 association, dissociation rates and O_2 affinity can also play an important role in determining HCO activity.

To investigate additional factors that determine HCO activity, we explored the role of heme $E°'$ in modulating rate constants of O_2 association (k_{on}), dissociation (k_{off}) and O_2 affinity. The k_{on} of O_2 binding to F33Y-Cu_BMb variants was measured using flow-flash technique wherein fully reduced CO-bound heme enzyme was mixed in a stopped-flow apparatus with oxygenated solution. The reaction was initiated by a short laser flash, breaking the photolabile Fe–CO bond, allowing binding of O_2 to be studied by time-resolved spectroscopy. We prepared CO-bound F33Y-Cu_BMb by reacting 5 μM of Fe^{2+} form mixed with 1.5 mM CO. The resulting complex exhibited UV-Vis signals at 422, 540 nm and 573 nm (Fig. S2), suggesting complete formation of the CO-adduct. The CO bound F33Y-Cu_BMb was then subjected to flash-photolysis and reacted with O_2 (Fig. 3A and S3). The reaction proceeded predominantly in a monophasic manner to reach heme-Fe(II)-O_2 state and subsequently studied as a function of O_2 concentration to obtain the second-order k_{on} for O_2 binding as 21 ± 2 mM^{-1} s^{-1} (Fig. 3B). Similar experiments when conducted with other F33Y-Cu_BMb variants obtained k_{on} as 48 ± 3 mM^{-1} s^{-1}, 70 ± 10 mM^{-1} s^{-1} and 250 ± 70 mM^{-1} s^{-1} for S92A-, (MF-heme) and (DF-heme) variants, respectively. Thus, increasing heme $E°'$ by ca. 210 mV results in 12-fold increase in k_{on} of the Mb-based HCO models (Fig. 3C). In addition to k_{on} for O_2, the observed rate constants for CO binding also increased systematically by ca. 21-fold upon increasing heme $E°'$ (Table S2 and Fig. S8B). The reason behind this consistent increase in O_2/CO binding rates with increasing $E°'$ can be explained by considering the electron density of heme iron. As the $E°'$ increases, electron density on heme iron decreases, which favors binding of electron donating ligands like O_2/CO and results in an increase in O_2/CO binding rate constants. To provide further support to this hypothesis, we surveyed literature for k_{on} of different HCO types and found that *R. sphaeroides cbb*$_3$ oxidase with low catalytic heme $E°'$ of −59 mV exhibits 10-fold slower O_2 association rates (k_{on} = 11,000 mM^{-1} s^{-1})[21,22] than *R. sphaeroides aa*$_3$ oxidase (k_{on} = 100,000 mM^{-1} s^{-1}) with heme $E°'$ of 220 mV.[22,23] Moreover, NO reductase (NOR from *P. denitrificans*) that also possess a low-potential heme *b*$_3$ ($E°'$ = 60 mV) and performs O_2-reduction cross-reactivity, binds O_2 with k_{on} of 25,000 mM^{-1} s^{-1} approximately 4-fold slower than *R. sphaeroides aa*$_3$ oxidase.[24] Therefore, a correlation between increased heme $E°'$ values and increased k_{on} for O_2 not only exists for Mb-based HCO models but native HCOs as well.

Next, we probed the impact of heme $E°'$ on O_2 dissociation of F33Y-Cu_BMb variants. The rates of O_2 dissociation (k_{off}) was extracted from the plot of observed rate constants for O_2 binding at different O_2 concentration using protocols reported previously (Fig. 3A, S5).[24] The k_{off} values were found to be 14 ± 1 mM^{-1} s^{-1}, 11 ± 2 mM^{-1} s^{-1}, 160 ± 10 mM^{-1} s^{-1}

and 500 ± 40 mM^{-1} s^{-1} for F33Y-Cu_BMb, S92A-, (MF-heme) and (DF-heme) variants respectively. Thus, k_{off} values for O_2 also increased with increasing $E^{\circ\prime}$ values (Fig. 3B). Specifically, the HCO model with highest $E^{\circ\prime}$ (F33Y-Cu_BMb(DF-heme)) displayed ca. 35-fold enhanced k_{off} than that of F33Y-Cu_BMb. To explain these observations, we probed the properties of O_2 bound to heme center using density functional theory (DFT). Quantum chemical DFT calculations were performed on three O_2–bound heme models: heme *b*, MF-heme and DF-heme, in which all porphyrin substituents were kept the same as in the native enzyme-based systems, except that the propionate group was replaced by methyl to facilitate the calculations. Since, O_2-bound heme is known to exist in resonance between its ferrous-oxy (Fe(II)-O_2) and ferric-superoxy (Fe(III)-O_2^-) forms, we investigated the electronic charge, spin densities and energy of both the structures. A comparison of charge densities within the three heme types showed that O_2 molecule becomes less negative as the heme $E^{\circ\prime}$ increases – The negative charge on O_2 of superoxy decreases from native heme (−0.152 e), MF-heme (−0.143 e) to DF-heme (−0.135 e). Even the charge on the O_2 molecule of oxy form became less negative with the addition of electron-withdrawing formyl groups (Table 1). These results suggest that electron-withdrawing substituents on porphyrin, as evident by higher $E^{\circ\prime}$, withdraw negative charge from O_2 fragment back to iron porphyrin as also shown by less positive iron charges in Table 1. This phenomenon makes O_2 closer to a neutral state for higher $E^{\circ\prime}$ values and thus, more prepared for faster dissociation. This computational trend is consistent with and explains the observed experimental O_2 dissociation rates for different F33Y-Cu_BMb variants.

Since the variation in heme $E^{\circ\prime}$ affects both k_{on} and k_{off} rates, we looked at its impact on O_2 affinity (K_d) of F33Y-Cu_BMb variants. F33Y-Cu_BMb was found to exhibit a K_d of 0.7 ±0.08 mM, which is 5-fold weaker than that of WTMb (K_d =0.14 mM). Thus, adding hydrophilic residues H43, H29 and Y33 close to catalytic heme reduced its affinity for non-polar hydrophobic oxygen. Similarly, increasing hydrophobicity by addition of S92A residue close to catalytic heme iron in S92A-F33Y-Cu_BMb (K_d =0.2 ±0.04 mM) increases the O_2 affinity of heme by 3.5-fold. Finally, F33Y-Cu_BMb (MF-heme) and F33Y-Cu_BMb (DF-heme) exhibit rather weak K_d values of 2.3 ±0.4 mM and 2.0±0.6 mM respectively. Thus, the two variants with high heme $E^{\circ\prime}$ reveal 3-fold lower O_2 affinity than parent F33Y-Cu_BMb explaining why an increase in their ET rates does not translate directly to an increased O_2 reduction rates. Overall, these results indicate that increasing heme $E^{\circ\prime}$ values leads to a decrease in O_2 affinity consistent with previous studies on Mb models that show electron-withdrawing fluoro-substituted hemes exhibiting low O_2 affinity values.[28] This observation is further corroborated with *R. sphaeroides* cbb_3 oxidase that exhibits the lowest heme $E^{\circ\prime}$ value of −59 mV and also displays the lowest K_m for O_2 (7 nM) among all oxidases.[29] This apparent high O_2 affinity of cbb_3 oxidase helps them cope with extremely low concentration of O_2 (3–22 nM) in root legumes. Thus, tuning heme $E^{\circ\prime}$ is an efficient method for HCOs to adapt to environmental constraints such as low O_2 concentration.

The complete reduction of O_2 to H_2O requires an efficient control of its ET, O_2 binding/dissociation rates and O_2 affinity. By employing a functional model of HCO with systematically tuned $E^{\circ\prime}$, we show that enzymes like HCOs use their heme $E^{\circ\prime}$ to control these parameters as well as the electronics of bound O_2. These results not only have significant impact in bioenergetics but also help understand how nature has fine-tuned $E^{\circ\prime}$

for various metalloproteins for their optimal function. In particular, heme proteins exhibit a wide variety of heme $E^{o'}$ (see Fig. S7 for few examples), and understanding the reason for this variation and associated implications on their enzymatic activity will help better understand the structure and reaction mechanism of these proteins.

Experimental Section

Experimental details pertaining to expression and purification of proteins, kinetic and computational measurements are detailed in the Supporting Information.

Supplementary Material

Refer to Web version on PubMed Central for supplementary material.

Acknowledgments

This report is based on work supported by a grant from the US National Institute of Health (GM062211) to YL and by a grant from the Faculty of Science at Stockholm University to PÄ. YZ acknowledges the partial support by an NSF grant CHE-1300912. AB-D thanks the financial support from Schlumberger foundation Faculty for the Future fellowship.

References

1. Bertini, IG., Lippard, HB., Valentine, JS. Bioinorganic Chemistry. University Science Books; Sausilito, CA: 1994.
2. Lippard, SJB. Principles of Bioinorganic Chemistry. University Science Books; Mill Valley, CA: 1994.
3. a) Ortiz de Montellano PM, Raven EL. Nat Prod Rep. 2007; 24:499.b) Lu Y. Angew Chem Int Ed. 2006; 45:5588.c) Lu Y, Yeung N, Sieracki N, Marshall NM. Nature. 2009; 460:855. [PubMed: 19675646] d) Petrik ID, Liu J, Lu Y. Curr Opin Chem Biol. 2014; 19:67. [PubMed: 24513641]
4. Babcock GT, Varotsis C, Zhang Y. Biochim Biophys Acta. 1992; 1101:192. [PubMed: 1321667]
5. Babcock GT, Wikström M. Nature. 1992; 356:301. [PubMed: 1312679]
6. Ferguson-Miller S, Babcock GT. Chem Rev. 1996; 96:2889. [PubMed: 11848844]
7. Garcia-Horsman JA, Barquera B, Rumbley J, Ma J, Gennis RB. J Bacter. 1994; 176:5587.
8. Ellis WR, Wang H, Blair DF, Gray HB, Chan SI. Biochemistry. 1986; 25:161. [PubMed: 3006749]
9. a) Karlin KD, Nanthakumar A, Fox S, Murthy NN, Ravi N, Huynh BH, Orosz RD, Day EP. J Am Chem Soc. 1994; 116:4753.b) Karlin KD, Fox S, Nanthakumar A, Murthy NN, Wei N, Obias HV, Martens CF. Pure Appl Chem. 2009; 67:289.
10. Kim E, Chufan EE, Kamaraj K, Karlin KD. Chem Rev. 2004; 104:1077. [PubMed: 14871150]
11. a) Raven EL. Heteroatom Chem. 2002; 13:501.b) Korendovych IV, Kulp DW, Wu Y, Cheng H, Roder H, DeGrado WF. Proc Natl Acad Sci USA. 2011; 108:6823. [PubMed: 21482808] c) Zastrow ML, Pecoraro VL. Coord Chem Rev. 2013; 257:2565. [PubMed: 23997273] d) Mocny CS, Pecoraro VL. Accts Chem Res. 2015; 48:2388.e) Makhlynets OV, Gosavi PM, Korendovych IV. Angew Chem Int Ed. 2016; 55:9017.f) Maeda Y, Makhlynets OV, Matsui H, Korendovych IV. Annu Rev Biomed Eng. 2016; 18:311. [PubMed: 27022702] g) Plegaria JS, Pecoraro VL. Meth Mol Biol. 2016; 1414:187.h) Bhagi-Damodaran A, Petrik ID, Lu Y. Isr J Chem. 2016; 56:773. [PubMed: 27994254]
12. a) Sigman JA, Kwok BC, Lu Y. J Am Chem Soc. 2000; 122:8192.b) Sigman JA, Kim HK, Zhao X, Carey JR, Lu Y. Proc Natl Acad Sci USA. 2003; 100:3629. [PubMed: 12655052]
13. Miner KD, Mukherjee A, Gao Y-G, Null EL, Petrik ID, Zhao X, Yeung N, Robinson H, Lu Y. Angew Chem Int Ed. 2012; 51:5589.

14. Yu Y, Mukherjee A, Nilges MJ, Hosseinzadeh P, Miner KD, Lu Y. J Am Chem Soc. 2014; 136:1174. [PubMed: 24383850]
15. Bhagi-Damodaran A, Petrik ID, Marshall NM, Robinson H, Lu Y. J Am Chem Soc. 2014; 136:11882. [PubMed: 25076049]
16. a) Lieber CM, Karas JL, Gray HB. J Am Chem Soc. 1987; 109:3778.b) Chang IJ, Gray HB, Winkler JR. J Am Chem Soc. 1991; 113:7056.c) Gray HB, Winkler JR. Ann Rev Biochem. 1996; 65:537. [PubMed: 8811189]
17. a) Xiong P, Nocek JM, Vura-Weis J, Lockard JV, Wasielewski MR, Hoffman BM. Science. 2010; 330:1075. [PubMed: 21097931] b) Trana EN, Nocek JM, Knutson AK, Hoffman BM. Biochemistry. 2012; 51(43):8542. [PubMed: 23067206] c) Jiang N, Kuznetsov A, Nocek JM, Hoffman BM, Crane BR, Hu X, Beratan DN. J Phys Chem B. 2013; 117(31):9129. [PubMed: 23895339]
18. a) Shifman JM, Gibney BR, Sharp RE, Dutton PL. Biochemistry. 2000; 39:14813. [PubMed: 11101297] b) Kennedy ML, Gibney BR. Curr Op Struc Biol. 2001; 11(4):485.c) Reedy CJ, Elvekrog MM, Gibney BR. Nucleic Acids Res. 2008; 36:307.
19. a) Yu Y, Cui C, Liu X, Petrik ID, Wang J, Lu Y. J Am Chem Soc. 2015; 137:11570. [PubMed: 26318313] b) Liu X, Yu Y, Zhang W, Lu Y, Wang J. Angew Chem Int Ed. 2012; 51:4312.c) Petrik ID, Davydov R, Ross M, Zhao X, Hoffman BM, Lu Y. J Am Chem Soc. 2016; 136:1134.
20. Mukherjee S, Mukherjee A, Bhagi-Damodaran A, Lu Y, Dey A. Nat Commun. 2015; 6:8467. [PubMed: 26455726]
21. Rauhamaki V, Bloch DA, Verkhovsky MI, Wikström M. J Biol Chem. 2009; 284:11301. [PubMed: 19252222]
22. Lee HJ, Gennis RB, Adelroth P. Proc Natl Acad Sci USA. 2011; 108:17661. [PubMed: 21997215]
23. Ädelroth P, Ek M, Brzezinski P. Biochim Biophys Acta Bioenerg. 1998; 1367:107.
24. Flock U, Watmough NJ, Ädelroth P. Biochemistry. 2005; 44:10711. [PubMed: 16060680]
25. De Angelis F, Jarzęcki AA, Car R, Spiro TG. J Phys Chem B. 2005; 109:3065. [PubMed: 16851321]
26. Ling Y, Zhang Y. Ann Rep Comp Chem. 2010; 6:65.
27. a) Chen H, Ikeda-Saito M, Shaik S. J Am Chem Soc. 2008; 130:14778. [PubMed: 18847206] b) Chen H, Ikeda-Saito M, Shaik S. J Am Chem Soc. 2008; 130:14778. [PubMed: 18847206]
28. Shibata T, Nagao S, Fukaya M, Tai H, Nagatomo S, Morihashi K, Matsuo T, Hirota S, Suzuki A, Imai K, Yamamoto Y. J Am Chem Soc. 2010; 132:6091. [PubMed: 20392104]
29. Ekici S, Pawlik G, Lohmeyer E, Koch HG, Daldal F. Biochim Biophys Acta. 2012; 1817(6):898. [PubMed: 22079199]

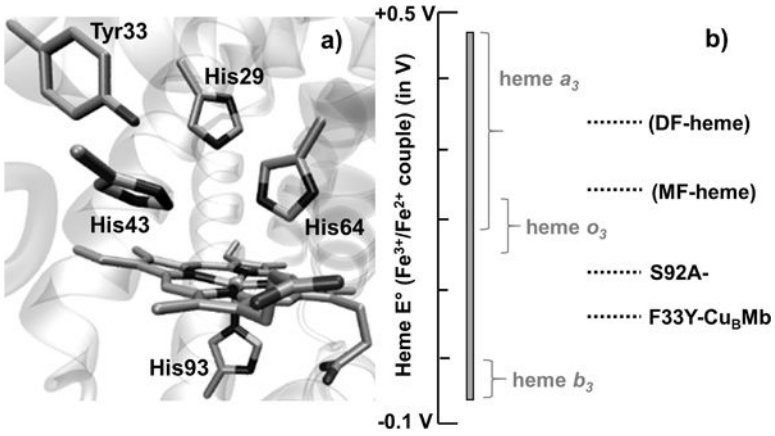

Figure 1.

a) Active site of F33Y-Cu_BMb showing heme *b* and side chains of His29, His43, His64, His93 and Tyr33. b) The heme $E°'$ range of HCOs that varies from −59 mV to 460 mV is represented as a grey bar while the curly brackets show heme cofactor type present in HCOs displaying those heme $E°'$ values. The heme $E°'$ of F33Y-Cu_BMb variants are shown as dotted black lines.

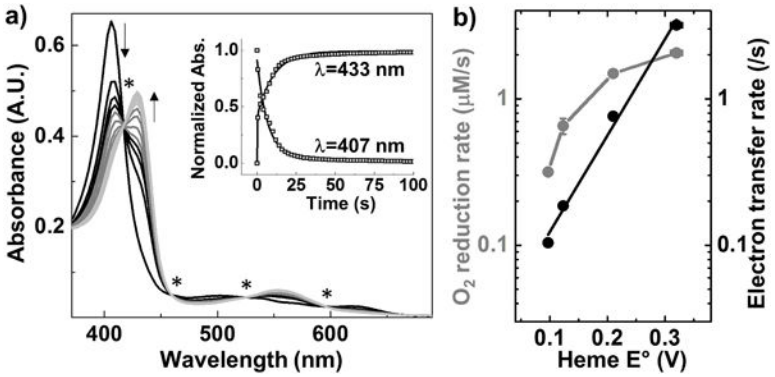

Figure 2.

a) Spectra obtained for 6 μM F33Y-Cu_BMb starting from Fe^{3+} form (black) going to Fe^{2+} form (grey). Isosbestic points are indicated by a star (*). Inset shows the variation in absorbance at 433 nm and 407 nm. b) Variation in oxidase activity (grey) and ET rates (black) for F33Y-Cu_BMb variants.

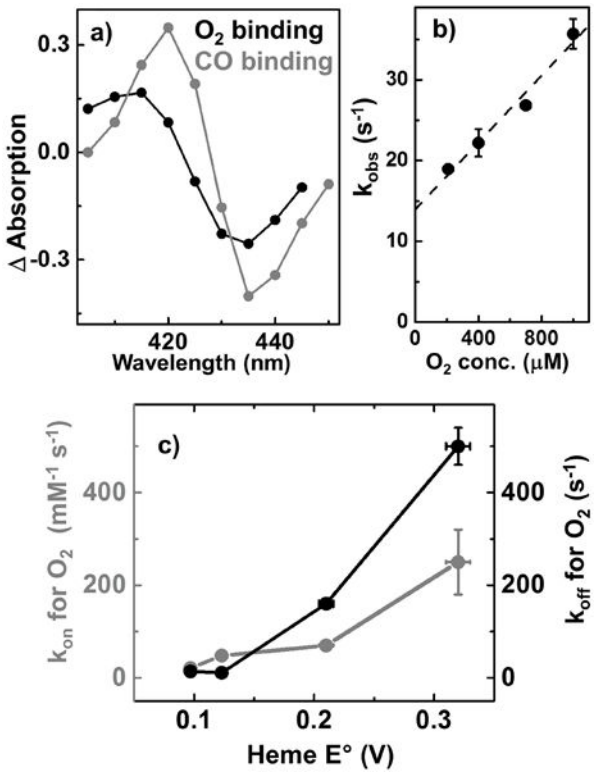

Figure 3.

a) Kinetic difference spectra for F33Y-Cu_BMb when heme binds O_2 (black) and CO (grey). b) Observed rate constant for O_2 binding as a function of O_2 concentration; the slope of this plot is used to calculate k_{on} for O_2 binding and the intercept is k_{off} for O_2 dissociation. c) Variation in k_{on} (grey) and k_{off} (black) for F33Y-Cu_BMb variants with tuned heme E°′.

Table 1

Variation in electronic charge on iron and O_2 molecule for heme-O_2 variants namely, Fe(II)-O_2 and Fe(III)-O_2^- forms

Sample	Q_{Fe} (e)	Q_{O2} (e)
heme-*b*-Fe^{2+}-O_2	1.950	−0.051
heme-*b*-Fe^{3+}-O_2^-	1.953	−0.152
MF-heme-Fe^{2+}-O_2	1.943	−0.044
MF-heme-Fe^{3+}-O_2^-	1.946	−0.143
DF-heme-Fe^{2+}-O_2	1.934	−0.034
DF-heme-Fe^{3+}-O_2^-	1.938	−0.135